Physica B 526 (2017) 96–101

Contents lists available at ScienceDirect

Physica B

journal homepage: www.elsevier.com/locate/physb

Electronic and phononic modulation of MoS_2 under biaxial strain

A. Moghadasi, M.R. Roknabadi*, S.R. Ghorbani, M. Modarresi

Department of Physics, Faculty of Science, Ferdowsi University of Mashhad, Mashhad, Iran

ARTICLE INFO

Keywords:
MoS_2
DFT
Phonon softening
Specific heat
2D material
Band gap engineering

ABSTRACT

Dichalcogenides of transition metals are attractive material due to its unique properties. In this work, it has been investigated the electronic band structure, phonon spectrum and heat capacity of MoS_2 under the applied tensile and compressive biaxial strain using the density functional theory. The Molybdenum disulfide under compressive (tensile) strain up to 6% (10%) has stable atomic structure without any negative frequency in the phonon dispersion curves. The tensile biaxial strain reduces the energy gap in the electronic band structure and the optical-acoustic gap in phonon dispersion curves. The tensile biaxial strain also increases the specific heat capacity. On the other hand, the compressive biaxial strain in this material increases phonon gap and reduces the heat capacity and the electronic band gap. The phonon softening/hardening is reported for tensile/compressive biaxial strain in MoS_2. We report phonon hardening for out of plane ZA mode in the presence of both tensile and compressive strains. Results show that the linear variation of specific heat with strain ($C_V \propto \varepsilon$) and square dependency of specific heat with the temperature ($C_V \propto T^2$) for low temperature regime. The results demonstrate that the applied biaxial strain tunes the electronic energy gap and modifies the phonon spectrum of MoS_2.

1. Introduction

Dichalcogenides of transition metals are receiving increasing interest from a wide range of scientific and technological fields due to their excellent material properties. Unlike the materials such as graphene, excellent properties of these materials make them useful as a replacement for silicon in the transistor channel due to the fact that they have a natural gap. Compared to other dichalcogenides of transition metals, molybdenum disulfide (MoS_2) have been widely studied, because the bulk abundantly found in nature. Molybdenum disulfide is a semiconductor with a honeycomb structure; in parallel with graphene, the material is formed of a molybdenum layer which is placed between two layers of sulfur and form a hexagonal structure. These layers are connected by covalent bonds and charge carriers can move between these layers, this property creates interesting electronic and mechanical properties in this material, and makes it ideal for application in devices such as transistors, super-lubricants [1], ultralow thermal conductivity devices [2] and solar cell converters [3]. High-quality crystals of this material have been developed by chemical vapor transport [4,5].

The monolayer and multi-layer thermal properties of MoS_2have also been studied and investigated experimentally and theoretically. Recently there has been growing effort on the synthesis of MoS_2 in laboratories [6–9].

The thermal behavior of materials is an interesting topic, both from scientific point of view as well as industrial applications. Liu et al. measured anisotropic thermal conductivity of bulk crystal and MoS_2 thin film using pump-probe technique based on magneto-optical Kerr effect [10]. Ghosh and Singisetti [11] calculated the thermoelectric transport coefficients of electrons in two dichalcogenides of transition metals i.e. MoS_2 and WS_2. They used the Boltzmann transport equation solution and coupled current (heat and electrical) equations, they also applied Rod's iteration technique. The Electron thermal conductivity in their calculations was very low while the decline in the value of the coefficient can be contributed to very high phonon thermal conductivity of the material. Zhang et al. [12] used non-equilibrium Green's function method, the first-principles calculations and molecular dynamics simulations to investigate the thermoelectric coefficients of hybrid nanoribbons of MoS_2/WS_2. Their results showed that hybrid nanoribbons had higher energy efficiency in comparison to the nanoribbons of MoS_2 and WS_2. Ding et al. [13] used non-equilibrium molecular dynamic simulation to investigate the effects of lattice defects and mechanical strain on the thermal conductivity of a monolayer molybdenum disulfide. Their results indicated that a small amount of lattice defects or a small amount of mechanical strain in a monolayer had a great effect on reducing the thermal conductivity of molybdenum disulfide. Using Boltzmann transport equation in the relaxation time approximation with the first-principles calculations, Saha and Mahapatra calculated the lattice heat capacity and thermal

* Corresponding author.
E-mail address: roknabad@um.ac.ir (M.R. Roknabadi).

http://dx.doi.org/10.1016/j.physb.2017.09.059
Received 27 June 2017; Received in revised form 7 September 2017; Accepted 15 September 2017
Available online 18 September 2017
0921-4526/

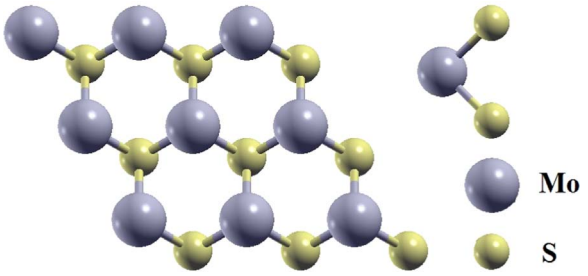

Fig. 1. The crystal structure of molybdenum disulfide from the top (left) and side (right) view.

conductivity of molybdenum disulfide. They recorded the lattice thermal conductivity at room temperature about 34.06 W m^{-1} K^{-1}[14].

In this study, the effect of applied biaxial strain on the thermal properties of MoS_2 have been investigated. The combination of Density Functional Theory (DFT) and Quasi-Harmonic Approximation (QHA) have been used to investigate the electronic and vibrational properties of MoS_2 under applied compressive and tensile biaxial strain. Moreover, the acoustic-optical phonon gap, phonon group velocity and specific heat capacity of MoS_2 have been studied under biaxial strain.

2. Computational and theoretical method

The molybdenum disulfide monolayer is a two-dimensional crystal with a hexagonal structure. The unit cell contains one molybdenum atom and two sulfur atoms. Molybdenum atoms are sandwiched between two layers of sulfur atoms as shown in Fig. 1.

We examined the electronic properties of MoS_2 in the DFT frame work. We applied different values of compressive and tensile biaxial strain to the MoS_2 monolayer. The biaxial strain is applied in both hexagonal lattice vectors which saves the hexagonal symmetry of crystal. First principle calculations are performed by using the quantum espresso package [15]. Electronic band structure and energy are calculated using the ab-initio calculations within the framework of Density Functional Theory (DFT). The ultra-soft pseudo-potential has been used to describe the core electron potentials. The cut-off energy for the plane wave expansion of wave function and charge density are set to 60 and 800 Ry, respectively. To avoid the interlayer interaction, 20 Angstrom distance perpendicular to the MoS_2 plane is considered. The first Brillouin zone is sampled in a 30 × 30 × 1 Monkhorst-Pack method [16]. For the atomic configuration relaxation, the maximum Hellmann-Feynman force on each atom is less than 0.00018 (Ry/au). The DFT parameters were increased to reach the convergence of final results. The phonon spectrum has been calculated by using the density functional perturbation theory [17]. Phonon dispersion spectrum has been calculated in a 3 × 3 × 1 uniform q-point grid. In addition, in order to calculate the thermal properties of molybdenum disulfide, the Quasi-Harmonic Approximation (QHA) has been used, which conduct the calculations to the first order of non-harmonic approximation [18]. The thermal properties were calculated by using the QHA code developed by Eyvaz Isaev and distributed as a part of Quantum Espresso package [15].

3. Results and discussion

Based on our calculations the lattice parameters of MoS_2 is 3.18 Å. This is in good agreement with previous reported results in the LDA [14] and GGA [19]. Monolayer molybdenum disulfide band structure is shown in Fig. 2. The MoS_2monolayer is a semiconductor with direct gap at the K point. The valence band maximum (VBM) and the conduction band minimum (CBM) are located at the Dirac points of the 1BZ. The direct gap is 1.703 eV, which agrees with previous reports [20–26]. In addition, the obtained amount of gap is the relative

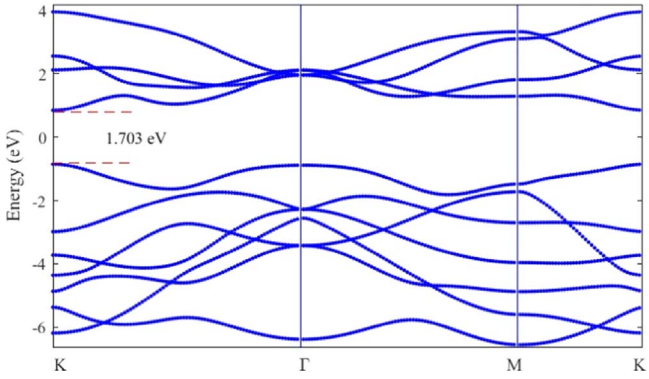

Fig. 2. The electronic band structure of molybdenum disulfide.

consistent with the results of other reports obtained by DFT [27,28]. Using of different potentials and approximations can be the reason of the small differences in the obtained amount of gap.

Generally, the application of compressive and tensile strain to the 2D plane changes the lattice constant and atomic overlap between adjacent atoms. This potentially may change different electronic and phononic properties of the 2D material. Based on the phonon spectrum calculations in the next section, the hexagonal MoS_2 is thermally stable under up to 6% (10%) of compressive (tensile) strain. Fig. 3 shows the electronic band structure of MoS_2 under different values of compressive and tensile strain.

Applying tension to this monolayer results in transfer of conduction and valence bands towards lower energies. This energy transfer is more tangible at the K points compared to the Γ point of the first Brillouin zone. This occurs in reverse order for MoS_2 under compressive strain. It means that applying compressive strain leads to transfer of energy bands towards higher energies.

Both compressive and tensile strain cause the direct to indirect electronic band gap transition. In the case of tensile strain the VBM and CBM are at Γand K points, respectively. It was found that the energy difference between VBM and the edge of valence bands at the Γ increases to higher value of tensile strain. In addition, the band width of the valence bands around the Fermi level increases by tensile strain which can be related to the increased overlap between Mo and S atoms inside the unit-cell. For the compressive strain the CBM is placed between Γ and K points. By increasing the tensile strain, the band gap decreases and the semiconductor-metal transition occurs at 10% of biaxial tensile strain. Fig. 4 shows the evaluation of monolayer molybdenum disulfide energy gap under biaxial pressure and tension. The values of band gap for tensile strain steadily decreases and the energy band gap reaches to less than zero at 10% of tensile strain. For the 10% strained MoS_2 the electronic energy gap is zero in resemblance to the 1T and 1T′ phases of MoS_2 [29]. At larger value of strain along the zigzag direction of MoS_2, the hexagonal to quadrilateral phase transition was observed by using the molecular dynamic [30]. Although for small value of compressive strain the energy gap increases slightly, then it decreases smoothly. Results are in well agreement with reported values for MoS_2 [23]. The same behavior was reported for other 2D materials [31–33]. The band gap engineering, in the 2D systems are crucial for extending the scope of their application, particularly in sensors and nano-electronics devices. The applied strain may result from the substrate effect. The external strain can be considered as the control and adjustment factors of the band gap in a monolayer molybdenum disulfide.

Beside the importance of the electronic structure, the thermal properties of solids are related to the atomic vibrations. To investigate the thermodynamic properties of strained MoS_2, we calculate all the vibration frequencies of MoS_2 under biaxial strain. Phonon dispersion curves of MoS_2 under biaxial pressure and tension up to 6% and 10% are shown in Fig. 5. The phonon spectrum includes three acoustic and

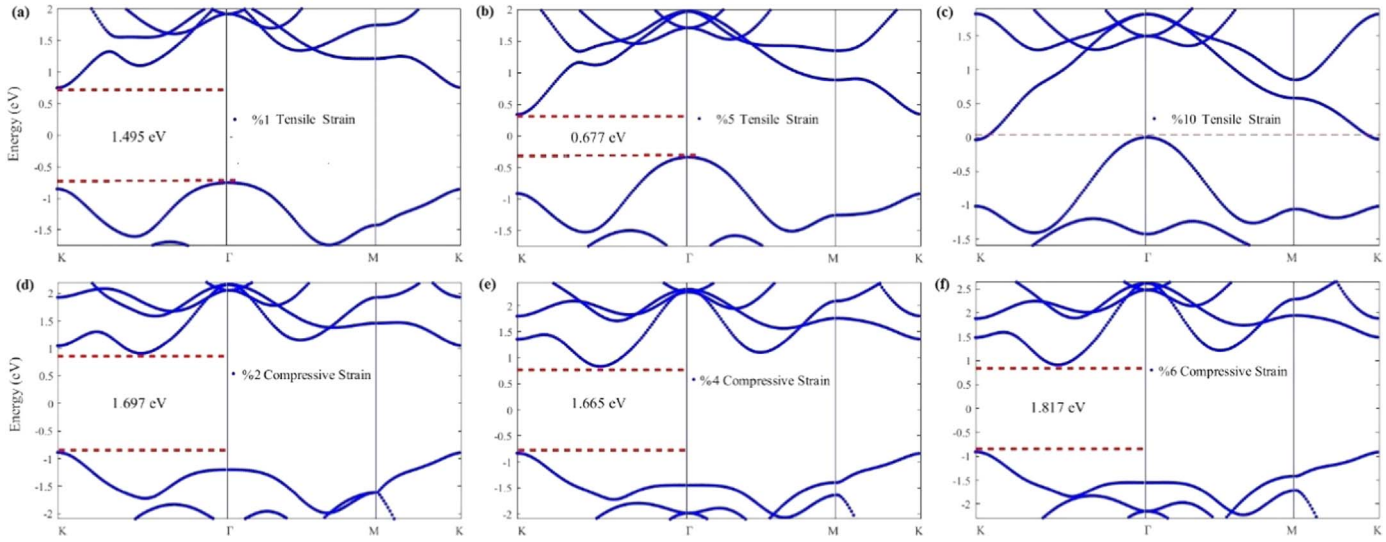

Fig. 3. Band structure and energy gap of molybdenum disulfide for a) 1%, b) 5% and c) 10% tensile strain and d) 2%, e) 4% and f) 6% compressive strain.

six optical branches which are determined in the Fig. 5a.

For the relaxed structure, the highest acoustic phonon frequency and the lower optical mode set at 235.4 (cm^{-1}) and 294.2 (cm^{-1}) respectively. The optical and acoustic branches are well separated by a phonon energy gap of around 57.71 cm^{-1} (577 meV).

Under applied tensile strain we observe the generally phonon softening in both optical and acoustic phonon branches of MoS_2. Moreover, the compressive strain leads to phonon hardening in all branches. The phonon softening in the strained graphene was observed experimentally using the Raman spectroscopy [34–36]. Also, the behavior of monolayer MoS_2 under the bi-axial tensile and compressive strain is similar to the graphene one under the uniaxial tensile and compressive strain [37]. The interesting point is related to the phonon hardening of ZA mode around the Gamma point for both tensile and compressive strains. This explains the stability of 2D material on the substrate which can be considered as external strain [38]. Our results suggest that the production of stabilized free-standing MoS_2 under applied strain due to the phonon hardening of soft ZA mode.

The applied strain changes the phonon energy gap between acoustic and optical branches. The values of phonon gap for different value of strain are presented in Fig. 6(a). For higher values of tensile strain the phonon gap decreases to reaches a value of 33.5 cm^{-1} at 10% of tensile strain.

The variation of phonon group velocity near the Γ point for LA, TA and ZA modes of MoS_2 under pressure and tension are shown in Fig. 6(b). For higher value of tensile strain, different acoustic modes get nearly same slope and the difference between group velocities of acoustic modes decreases. The phonon group velocity trend is different for each acoustic branch. The phonon velocity of ZA mode is minimum for the relaxed structure. For the LA mode, the phonon group velocity generally increases by decreasing the crystal volume. The group velocity in TA mode, remains almost constant as tensile and compressive strain increase. The variation of phonon group velocity by applied strain, suggests the heat transport modulation by external strain in MoS_2.

For relaxed structure, different acoustic modes are well separated around the Γ point. By applying tensile strain the separation between ZA and TA modes is disappeared between Γ and K points and the behavior of ZA mode changes from quadratic (k^2) to linear (k) for strain higher than 4%. The same behavior was reported for the out of plane mode in graphene under strain [39].

Fig. 7 shows the phonon frequency of optical and acoustic phonon branches at the K, Γ and M as high symmetry points of 1BZ.

Generally, the effect of strain is negligible for acoustic branches. However, as the phonon frequency for optical branches are increased, the phonon vibration frequencies are changed under an almost linear dependency of strain. At the K point, the energy difference between different optical phonon branches is decreased for high value of tensile strain.

Fig. 8 shows the variation of specific heat with temperature. For high temperature range, the value of specific heat for all strain values reaches to the classical independent temperature limit which is known

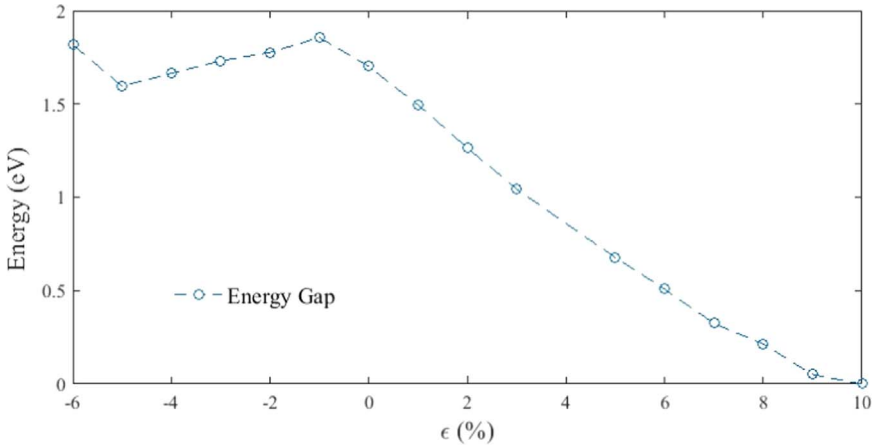

Fig. 4. The size of the band gap in different tensions and pressures (from 6% to 10% of the initial value of lattice parameter).

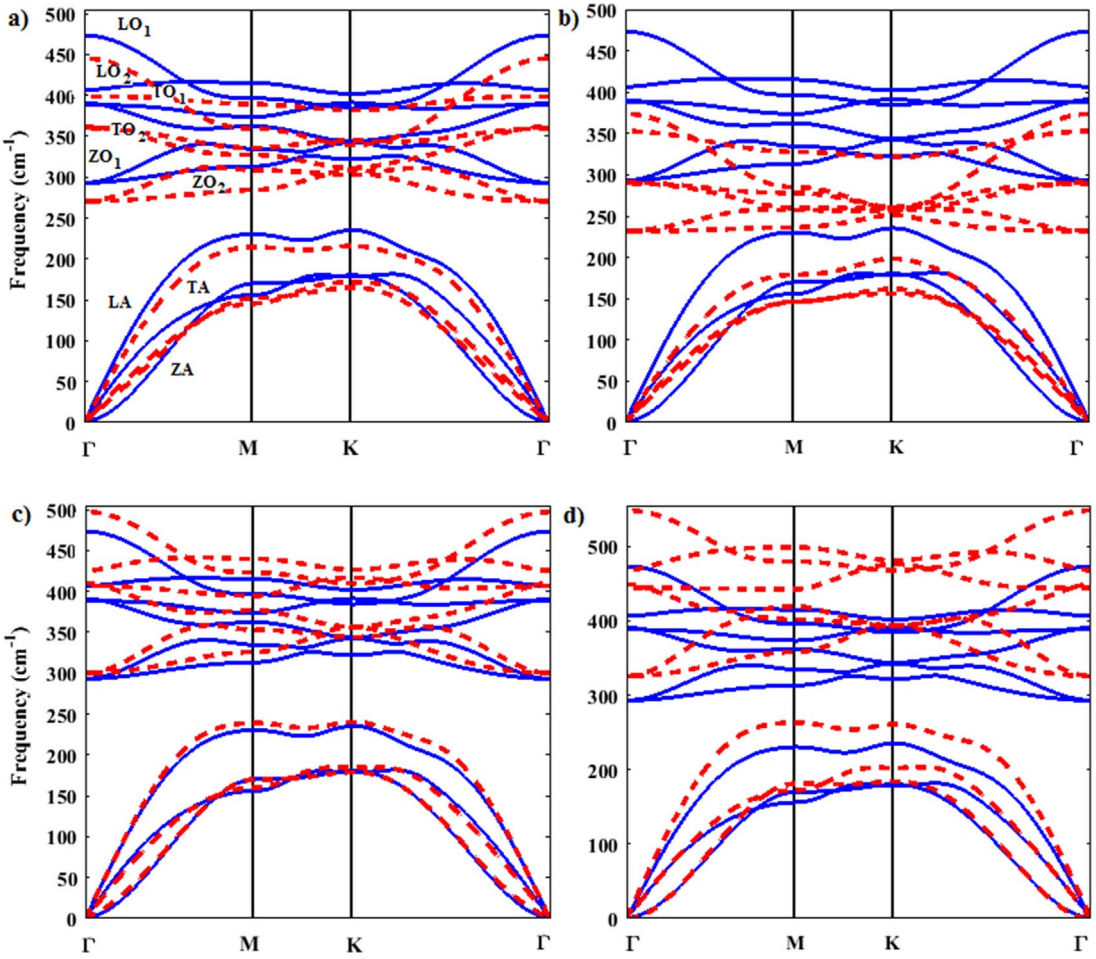

Fig. 5. The phonon dispersion curves of monolayer molybdenum disulfide under biaxial tension the comparison between relaxed atomic structure (line curve) and a) 4% tensile strain, b) 10% tensile strain, c) 2% compressive strain d) 6% compressive strain (dash curve).

as the Dulong–Petit law.

The applied biaxial strain modifies the heat capacity of MoS_2. The tensile strains of ten phonon modes and ease phonon excitation in the MoS_2 monolayer. As a result, the phonon contribution in the specific heat increases. On the other hand, the compressive strain decreases phononic specific heat due to the phonon hardening. For the low temperature limit we fit the specific heat data to the T^2function, as shown in the inset of Fig. 8(a). This is in contrast to the expected T^3 behavior of ordinary three-dimensional materials.

These variation of single-layer MoS_2 phonon frequencies under a bi-axial strain is similar to single layer graphene under a uniaxial strain. As a result, the increase of tensile/Compressive strain causes the phonon frequencies shift to lower/higher frequencies. Also, the increase of tensile/compressive strain increases/decreases the heat

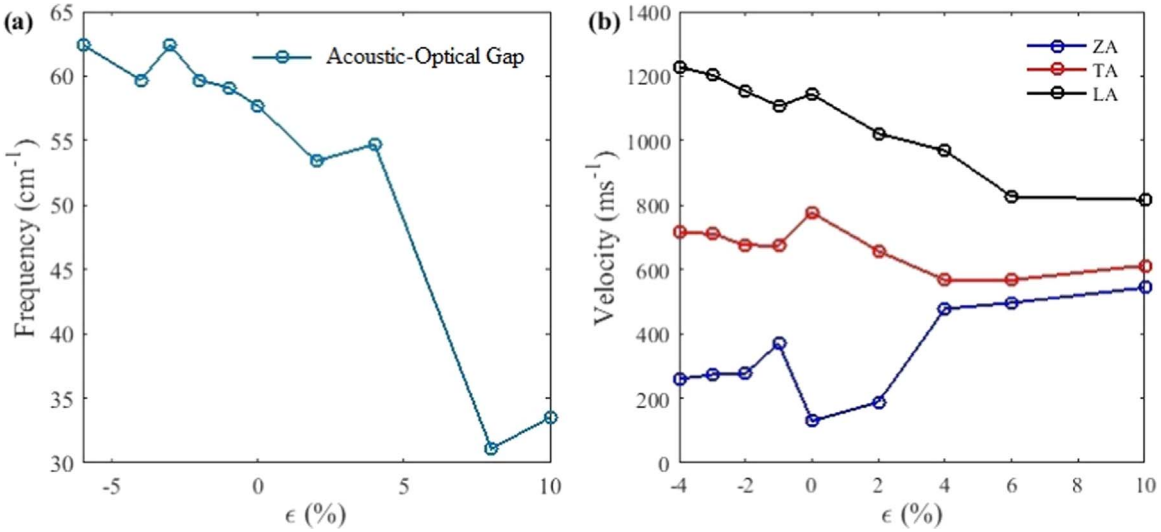

Fig. 6. The variation of a) acoustic-optical gap of phonon dispersion and b) the phonon group. velocity near the Γ point of first Brillouin zone of MoS_2 under pressure and tension.

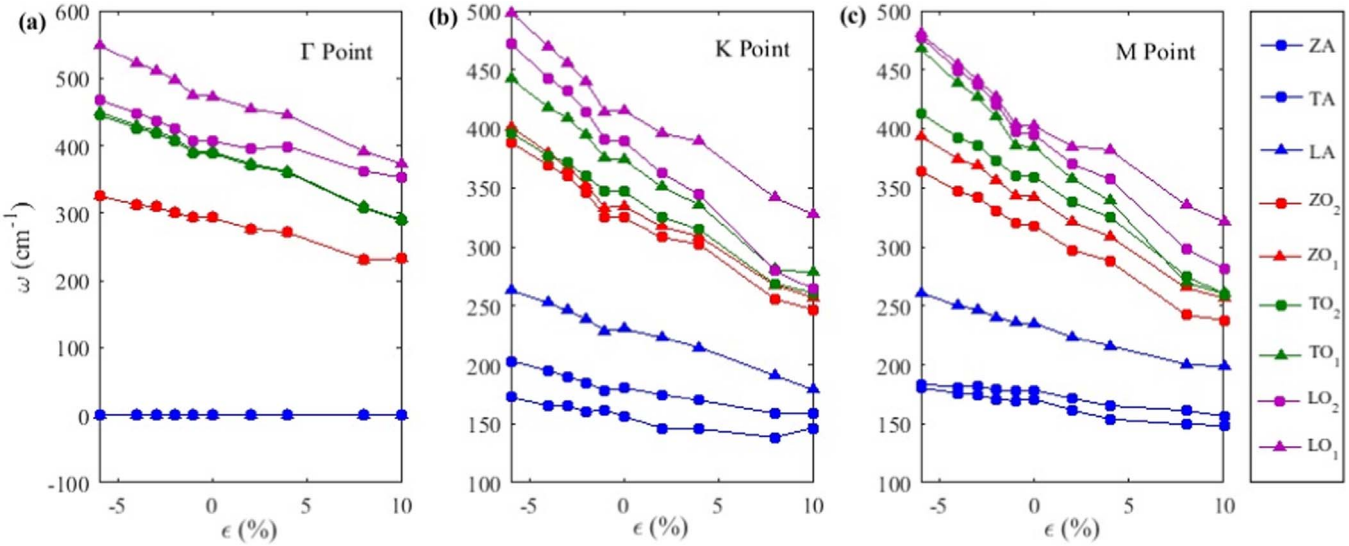

Fig. 7. The acoustic and optical phonon branches under pressure and tension at the a) Γ, b) K, c) M points.

capacity of the single-layer $MoS_2$with respect to the non-strain structure at higher temperatures (T > 350 K) [37].

In order to provide deeper insight into strain effect, the specific heat for different temperatures are presented as a function of strain in Fig. 9.

Next, to investigate the variation of specific heat with applied strain, the C_V in terms of the amount of applied strain to the sample at different temperatures are illustrated; the changes are fairly linear with strain. The specific heat variation is fitted to the $C_V = \beta\varepsilon + \text{const.}$ function. The values of βare presented in the Fig. 9. As temperature increases, the heat capacity slope (β) increases from 0.012 for 30 K to 0.11 for 100 K, then it decreases to 0.03 for 500 K. Increased temperature reduces heat capacity graph slope, i.e. at higher temperatures, heat capacity shows small changes to the tension and pressure. The linear variation of specific heat with applied strain is an experimental challenge for future works. The same linear variation of heat capacity with strain is reported for group four 2D nano-materials. In contrary, the heat capacity of silicene decreases with strain [38]. The electronic band energy gap engineering is essential for electronic devices. In addition, strained MoS_2 shows appropriate modulation on the vibration properties and specific heat which are essential for thermal management [40,41] of next generation Nano-electronic devices.

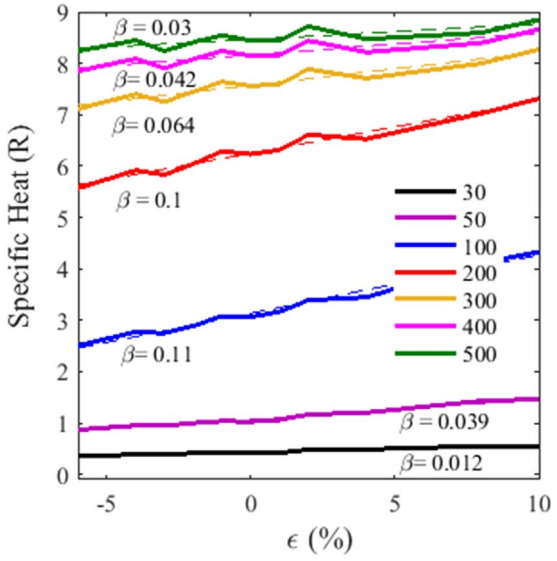

Fig. 9. The heat capacity of MoS_2in terms of tension and pressure applied to the sample at different temperatures. (dashed lines show linear fit of each graph).

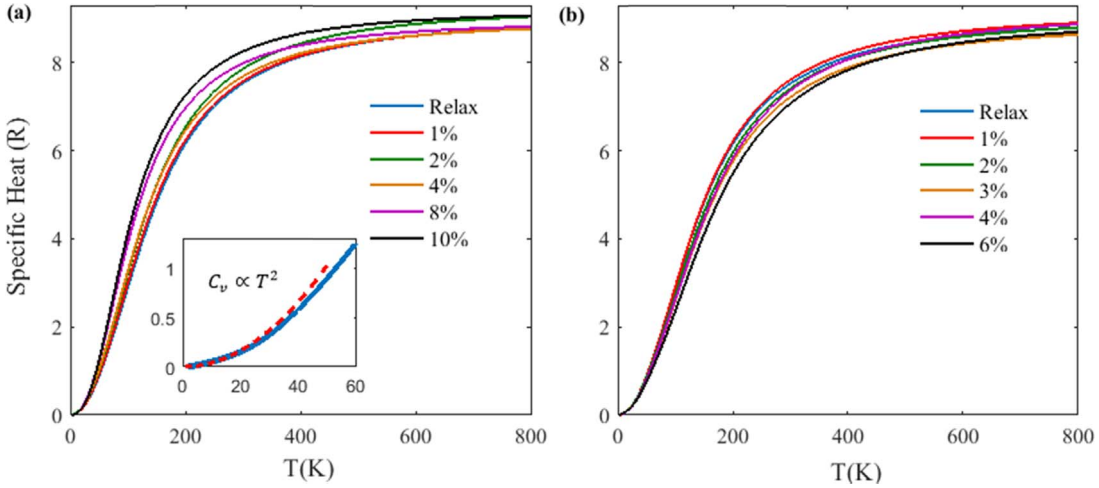

Fig. 8. Specific heat capacity in terms of international constant R a) for up to 10%tensile b) for up to 6% compressive. Inset: Specific heat capacity in low temperature.

4. Conclusion

In summary, a DFT study of electronic, vibration and specific heat modulation of MoS_2 under applied biaxial tensile and compressive strain is presented. Our results show that the applied strain, controls the electronic and photonic band gap of monolayer MoS_2. The strained MoS_2 shows the phonon softening and phonon hardening for biaxial tensile and compressive strain, respectively. For the ZA mode the phonon hardening occurs for both negative and positive strains. The biaxial strain has different effect on the phonon group velocity around the Γ point for LA, TA and ZA branches. Moreover, it was found that specific heat shows the linear response to applied strain for a specific temperature and square dependency to the temperature at low temperature regime.

Acknowledgments

This work was supported by the Ferdowsi University of Mashhad (Grant no. .3.42507). A. Moghadasi thanks Dr. Azra Feyzi for fruitful discussion during the project.

References

[1] C. Lee, et al., Frictional characteristics of atomically thin sheets, Science 328 (5974) (2010) 76–80.
[2] C. Chiritescu, et al., Ultralow thermal conductivity in disordered, layered WSe2 crystals, Science 315 (5810) (2007) 351–353.
[3] J. Puthussery, et al., Colloidal iron pyrite (FeS2) nanocrystal inks for thin-film photovoltaics, J. Am. Chem. Soc. 133 (4) (2010) 716–719.
[4] A. Ubaldini, E. Giannini, Improved chemical vapor transport growth of transition metal dichalcogenides, J. Cryst. Growth 401 (2014) 878–882.
[5] A. Ubaldini, et al., Chloride-driven chemical vapor transport method for crystal growth of transition metal dichalcogenides, Cryst. Growth Des. 13 (10) (2013) 4453–4459.
[6] Y. Gong, et al., Tellurium-assisted low-temperature synthesis of MoS2 and WS2 monolayers, ACS Nano 9 (12) (2015) 11658–11666. http://dx.doi.org/10.1021/acsnano.5b05594.
[7] H. Li, et al., Synthesis and characterization of vertically standing MoS2 nanosheets, Sci. Rep. (2016) 6.
[8] A.M. Van Der Zande, et al., Grains and grain boundaries in highly crystalline monolayer molybdenum disulphide, Nat. Mater. 12 (6) (2013) 554–561.
[9] J.M. Woods, et al., One-step synthesis of MoS2/WS2 layered heterostructures and catalytic activity of defective transition metal dichalcogenide films, ACS Nano (2016).
[10] J. Liu, G.-M. Choi, D.G. Cahill, Measurement of the anisotropic thermal conductivity of molybdenum disulfide by the time-resolved magneto-optic Kerr effect, J. Appl. Phys. 116 (23) (2014) 233107.
[11] K. Ghosh, U. Singisetti, Thermoelectric transport coefficients in mono-layer MoS2 and WSe2: role of substrate, interface phonons, plasmon, and dynamic screening, J. Appl. Phys. 118 (13) (2015) 135711.
[12] Z. Zhang, et al., A theoretical prediction of super high-performance thermoelectric materials based on MoS2/WS2 hybrid nanoribbons, Sci. Rep. (2016) 6.
[13] Z. Ding, et al., Manipulating the thermal conductivity of monolayer MoS2 via lattice defect and strain engineering, J. Phys. Chem. C 119 (28) (2015) 16358–16365.
[14] D. Saha, S. Mahapatra, Analytical insight into the lattice thermal conductivity and heat capacity of monolayer MoS2, Phys. E: Low-Dimens. Syst. Nanostruct. 83 (2016) 455–460.
[15] P. Giannozzi, et al., QUANTUM ESPRESSO: a modular and open-source software project for quantum simulations of materials, J. Phys.: Condens. Matter 21 (39) (2009) 395502.
[16] H.J. Monkhorst, J.D. Pack, Special points for Brillouin-zone integrations, Phys. Rev. B 13 (12) (1976) 5188.
[17] S. Baroni, et al., Phonons and related crystal properties from density-functional perturbation theory, Rev. Mod. Phys. 73 (2) (2001) 515.
[18] S. Baroni, P. Giannozzi, E. Isaev, Thermal Properties of Materials from Ab-initio Quasi-harmonic Phonons, arXiv preprint arXiv:1112.4977, 2011.
[19] X. Fan, et al., Structural stability of single-layer MoS2 under large strain, J. Phys.: Condens. Matter 27 (10) (2015) 105401.
[20] H. Chermette, et al., Lubricating properties of molybdenum disulphur: a density functional theory study, Surf. Sci. 472 (1) (2001) 97–110.
[21] S. Han, et al., Band-gap transition induced by interlayer van der Waals interaction in MoS2, Phys. Rev. B 84 (4) (2011) 045409.
[22] P. Johari, V.B. Shenoy, Tuning the electronic properties of semiconducting transition metal dichalcogenides by applying mechanical strains, ACS Nano 6 (6) (2012) 5449–5456.
[23] P. Lu, et al., Strain-dependent electronic and magnetic properties of MoS2 monolayer, bilayer, nanoribbons and nanotubes, Phys. Chem. Chem. Phys. 14 (37) (2012) 13035–13040.
[24] G. Plechinger, et al., Raman spectroscopy of the interlayer shear mode in few-layer MoS2 flakes, Appl. Phys. Lett. 101 (10) (2012) 101906.
[25] E. Ridolfi, et al., A tight-binding model for MoS2 monolayers, J. Phys.: Condens. Matter 27 (36) (2015) 365501.
[26] E. Scalise, et al., Strain-induced semiconductor to metal transition in the two-dimensional honeycomb structure of MoS2, Nano Res. 5 (1) (2012) 43–48.
[27] E.S. Kadantsev, P. Hawrylak, Electronic structure of a single MoS 2 monolayer, Solid State Commun. 152 (10) (2012) 909–913.
[28] A. Kumar, P. Ahluwalia, Mechanical strain dependent electronic and dielectric properties of two-dimensional honeycomb structures of MoX2 (X = X = S, Se, Te), Phys. B: Condens. Matter 419 (2013) 66–75.
[29] Y. Liu, et al., First-principles study on structural, thermal, mechanical and dynamic stability of T′-MoS2, J. Phys.: Condens. Matter 29 (9) (2017) 095702.
[30] H. Bao, et al., Tensile loading induced phase transition and rippling in single-layer MoS2, Appl. Surf. Sci. 404 (2017) 180–187.
[31] R.G. Amorim, et al., Strain-and electric field-induced band gap modulation in nitride nanomembranes, J. Phys.: Condens. Matter 25 (19) (2013) 195801.
[32] D. Çakır, H. Sahin, F.M. Peeters, Tuning of the electronic and optical properties of single-layer black phosphorus by strain, Phys. Rev. B 90 (20) (2014) 205421.
[33] M.-Y. Liu, et al., Unexpected electronic structure of the alloyed and doped arsenene sheets: first-principles calculations, Sci. Rep. (2016) 6.
[34] M.A. Bissett, M. Tsuji, H. Ago, Strain engineering the properties of graphene and other two-dimensional crystals, Phys. Chem. Chem. Phys. 16 (23) (2014) 11124–11138.
[35] M. Huang, et al., Phonon softening and crystallographic orientation of strained graphene studied by Raman spectroscopy, Proc. Natl. Acad. Sci. 106 (18) (2009) 7304–7308.
[36] C. Si, Z. Sun, F. Liu, Strain engineering of graphene: a review, Nanoscale 8 (6) (2016) 3207–3217.
[37] M. Xia, S. Zhang, Modulation of specific heat in graphene by uniaxial strain, Eur. Phys. J. B – Condens. Matter Complex Syst. 84 (3) (2011) 385–390.
[38] Y.D. Kuang, et al., Tensile strains give rise to strong size effects for thermal conductivities of silicene, germanene and stanene, Nanoscale 8 (6) (2016) 3760–3767.
[39] K. Tada, et al., Modulations of thermal properties of graphene by strain-induced phonon engineering, Jpn. J. Appl. Phys. 56 (2) (2017) 025102.
[40] J.D. Renteria, D.L. Nika, A.A. Balandin, Graphene thermal properties: applications in thermal management and energy storage, Appl. Sci. 4 (4) (2014) 525–547.
[41] M. Shtein, et al., Graphene-based hybrid composites for efficient thermal management of electronic devices, ACS Appl. Mater. Interfaces 7 (42) (2015) 23725–23730.